

## 1. Introduction

The goal of these experiments is to examine dynamic performances of a digitally regulated speed servomechanism using computer simulations in MATLAB. There are 9 simulation experiments which allow the analysis of the influence of parameters of system and regulator to the character and accuracy of regulated speed and to the robustness of the system to the influence of disturbances.

## 2. Assignment of experiment

In this section the possible experiments are described. In the following, the SIMULINK models *A.mdl*, *B.mdl* and *C.mdl* are used. Instructions for the creation of models *B.mdl* and *C.mdl* are given in Section 4.

A. Run SIMULINK model *A.mdl* (see Section 4.1).

A1. Simulate the response of speed-controlled servomechanism to the step input  $\omega_{ref} = 40 \text{ rad/s}$ , at the constant load moment  $T_L = 5 \text{ Nm}$ . Assume that the reference input starts at  $t_1 = 0.01 \text{ s}$ , and the effect of disturbance at  $t_2 = 0.05 \text{ s}$ . Show the result of simulation on Fig. A1. Observe the waveforms on Fig. A1, determine the transition time of start-up and reduction of speed when load moment is in effect. Put obtained values in a Table A1.

A2. Repeat the experiment A1 for step input  $\omega_{ref} = 100 \text{ rad/s}$ . Show the result of simulation on Fig. A2. Determine the transition time of start-up and reduction of speed when load moment is in effect. Put obtained values in a Table A2. Compare values from Tables A1 and A2. Discuss obtained results.

A3. Simulate the response of speed-controlled servomechanism to the step input  $\omega_{ref} = 40 \text{ rad/s}$ , without load. Assume that the reference input starts at  $t_1 = 0.01 \text{ s}$ . Show the result of simulation on Fig. A3. Observe the ripple in the waveforms of drive moment. Calculate (in %) the ratio of peak-to-peak value of moment ripple  $\Delta m$  and maximally permitted moment  $T_{\max} = 10 \text{ Nm}$ . Put the values of parameters of speed regulator ( $K_p$ ,  $K_i$ ) and computed value of  $\Delta m$  [%] into Table A3.

A4. Retaining the same value of the parameter  $K_i$ , determine the value of parameter  $K_p$  so that the moment ripple be  $\Delta m \leq 10\%$ . Put obtained value in Table A4. Repeat the experiment A3, for values of the parameters from Table A4. Show the result in Fig. A4.

A5. Observe the character of the response of drive moment and speed in Fig. A4. Retaining the same value of parameter  $K_p$ , determine the value of parameter  $K_i$  so that the speed response be critically damped. Put obtained value into Table A5. Repeat the experiment A3, for values of the parameters from Table A5. Show the result in Fig. A5.

- B. Starting from SIMULINK model *A.mdl* make SIMULINK model *B.mdl*, so that an electromagnetic resolver with synchroconverter (with bandwidth  $f_{bw} = 1 \text{ kHz}$  and 12 bits resolution of position measurement) is used as sensor instead of an optical encoder. The instructions for creating the command file *startB.m* and model *B.mdl* are given in Section 4.2.

Run SIMULINK model *B.mdl*.

- B1. Simulate the response of speed-controlled servomechanism to the step input  $\omega_{ref} = 40 \text{ rad/s}$ , at the constant load moment  $T_L = 5 \text{ Nm}$ . Assume that the reference input starts at  $t_1 = 0.01 \text{ s}$ , and the effect of disturbance at  $t_2 = 0.05 \text{ s}$ . Show the result of simulation on Fig. B1. Observe the waveforms on Fig. B1, determine the transition time of start-up and reduction of speed when load moment is in effect. Put obtained values in a Table B1.

- B2. Repeat the experiment B1 for step input  $\omega_{ref} = 100 \text{ rad/s}$ . Show the result of simulation on Fig. B2. Determine the transition time of start-up and reduction of speed when load moment is in effect. Put obtained values in a Table B2. Compare values from Tables A1 and A2 and Tables B1 and B2. Discuss obtained results.

- C. Starting from SIMULINK model *B.mdl* make SIMULINK model *C.mdl*, which takes into account the elastic coupling between electrical drive and load. The parameters of mechanical subsystem with elastic coupling are given in Table 1.

Table 1. Parameters of mechanical subsystem with elastic coupling.

$J_m$ [kgm <sup>2</sup> ]	$F_m$ [Nms/rad]	$K_o$ [Nm/rad]	$J_L$ [kgm <sup>2</sup> ]	$F_L$ [Nms/rad]
0.0008	0.002	350	0.0002	0.002

The instructions for creating the command file *startC.m* and model *C.mdl* are given in Section 4.3.

Run SIMULINK model *C.mdl*.

- C1. Simulate the response of speed-controlled servomechanism to the step input  $\omega_{ref} = 40 \text{ rad/s}$ , at the constant load moment  $T_L = 5 \text{ Nm}$ . Assume that the reference input starts at  $t_1 = 0.01 \text{ s}$ , and the effect of disturbance at  $t_2 = 0.05 \text{ s}$ . Show the result of simulation on Fig. C1. Observe the waveforms on Fig. C1, determine the transition time of start-up and reduction of speed when load moment is in effect. Put obtained values in a Table C1. Discuss obtained results.

- C2. Observing the waveforms in Fig. C1, note the character of the speed during start up (when reference input is in effect) and when disturbance is in effect. Can you explain the differences in transition processes in these two cases

### 3. Theoretical background

In this section, the theoretical background necessary for understanding and successful realization of experiment is given. The structural synthesis of digitally speed-controlled servomechanism is shown which includes imperfections of:

- Mechanical subsystem,
- Electrical subsystem
- Sensor for measuring position.

Each component of speed-controlled servomechanism has corresponding SIMULINK model. The obtained model of digital speed-controlled loop is used as a base for performing procedure of optimal adjustment of parameters of speed regulator.

#### 3.1 The components of speed-controlled servomechanism

The speed-controlled servomechanism is a regulation system with speed-controlled closed loop feedback, which uses electrical drive as the executive organ. Its task is to provide the high quality control of speed of electrical drive in all working regimes. This means control that provides desired character of speed in transitional regime, high accuracy in steady state conditions and low sensitivity of regulated speed to the influence of disturbances. There are a lot of applications that require this type of control. In industry, the speed-controlled servomechanisms are used as executive organs in machine tools, robot mechanisms, assembly lines, heating, ventilation and climatization systems, etc.

The block diagram of the structure of a digitally speed-controlled servomechanism is shown in Fig.1. It consists of:

- Mechanical subsystem: Electrical drive (M), which is by elastic coupling coupled (S) to load (L) – most often a system of rotated masses.
- Electrical subsystem: Drive converter (P) and electrical drive (M) as the actuator of electromagnetic moment.
- Sensor (D) for measuring position.
- Block for speed measurement (MB)
- Speed regulator (REG) with limiter of reference moment (GM)

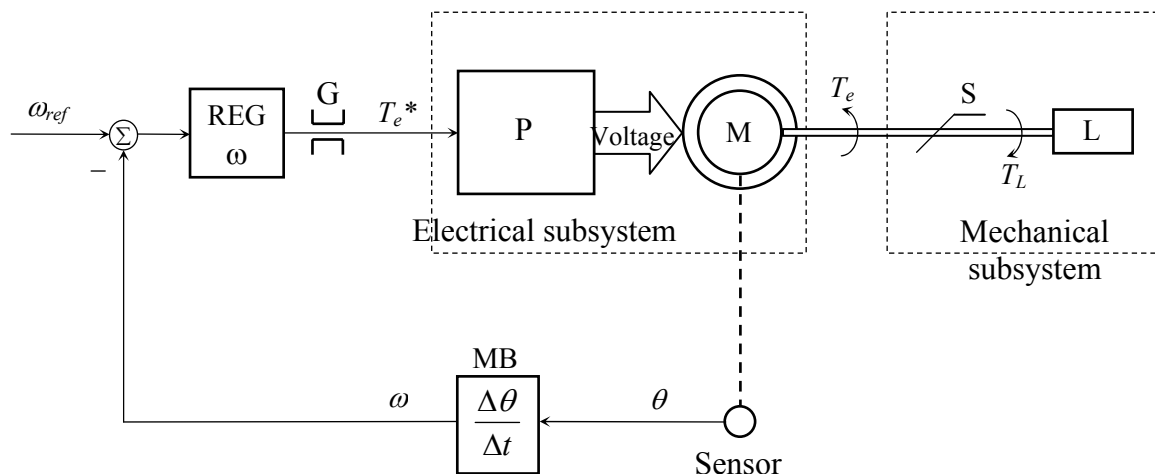


Fig. 1.

In Fig. 1 the following notation is used:

$\omega_{ref}$	reference speed
$T_e^*$	reference moment
$T_e$	output moment of electrical drive
$T_L$	load moment
$\theta$	position of shaft of electrical drive
$\omega$	angular speed of shaft rotation

Drive converter (P) generates voltage at the connection ends of an electrical drive (M) so that the output moment  $T_e$  tracks given reference input  $T_e^*$ . Through elastic coupling (S), the output moment  $T_e$  is carried to load where it produces rotational movement of system of rotational masses (L). The position of shaft  $\theta$  of the drive is measured using sensor (D). This information is used in the block for speed measurement (MB) for the estimation of angular speed  $\omega$ . In the error discriminator, the reference input  $\omega_{ref}$  is compared with the estimated angular speed  $\omega$ . The obtained error signal is fed to the input of the regulator (REG) which task is to generate reference moment  $T_e^*$  so that regulated speed tracks reference input.

In the following sections, the operation principles of components of a digitally speed-controlled servomechanism are presented, which take into account imperfections that will be modeled and considered during the choice of parameters of speed regulator.

### 3.2 Mechanical subsystem

The mechanical subsystem of a speed-controlled servomechanism consists of:

- Electrical drive (M)
- Elastic coupling (S)
- Load (L) – most often a system of rotated masses

Without loss of generality, it can be considered that the coupling (S) is a relatively long shaft having finite stiffness  $K_o$ . In this case, the mechanical subsystem having elastic coupling can be shown as in Fig. 2

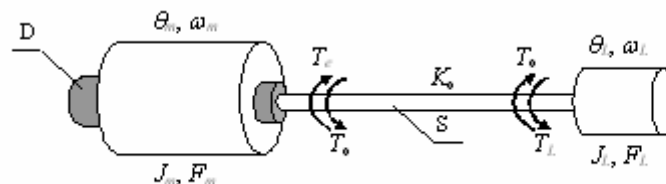


Fig. 2

In Fig. 2 the following notation is used:

$J_m, F_m$	moment of inertia and friction of electrical drive
------------	--

$\omega_m, \theta_m$	angular speed and position of shaft at the drive side
$T_o$	moment of the shaft
$\omega_L, \theta_L$	angular speed and position of shaft at the load side
$J_L, F_L$	moment of inertia and friction of load

### 3.2.1 Modeling of the mechanical subsystem in SIMULINK

The mechanical subsystem shown in Fig. 2 can be described by a system of equations:

$$J_m \ddot{\theta}_m = T_e - F_m \omega_m - T_o, \quad (1)$$

$$J_L \ddot{\theta}_L = T_o - F_L \omega_L - T_L, \quad (2)$$

$$T_o = K_o (\theta_m - \theta_L), \quad (3)$$

where,

$$\omega_m = \dot{\theta}_m \text{ and } \omega_L = \dot{\theta}_L. \quad (4)$$

The moment of the shaft  $T_o$  at the drive side (M) performs as load moment, and at the load side (L) as the drive moment. In the s-domain, the structure shown in Fig. 3 corresponds to the equations (1)-(4).

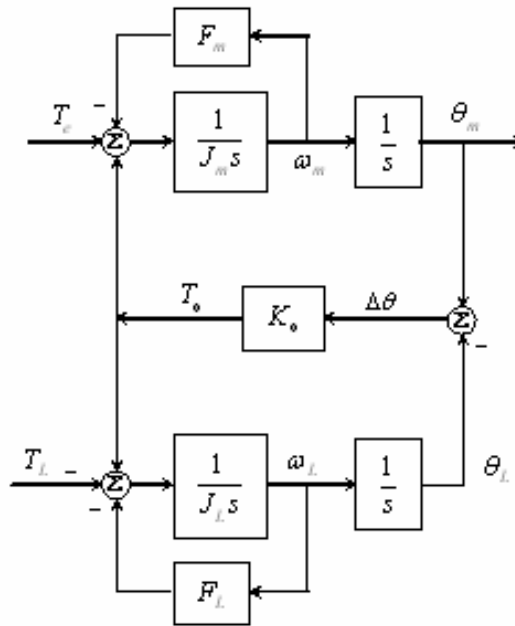


Fig. 3.

The structure shown in Fig. 3 corresponds to the SIMULINK model shown in Fig. 3a.

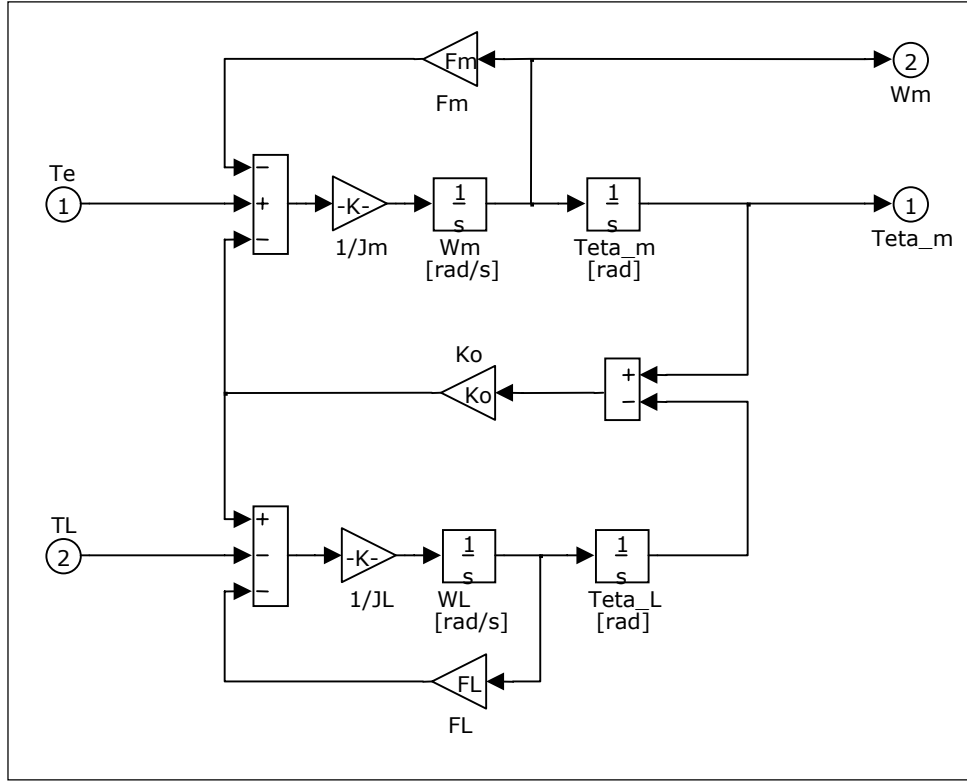


Fig. 3a.

The transfer function of the mechanical subsystem on Fig. 3, from input  $T_e$  to output  $\theta_m$ , at  $T_L = 0$ , is given by:

$$\frac{\theta_m(s)}{T_e(s)} = \frac{J_L s^2 + F_L s + K_o}{J_L J_m s^4 + (J_L F_m + J_m F_L) s^3 + (J_m K_o + F_m F_L + J_L K_o) s^2 + (F_m + F_L) K_o s}. \quad (5)$$

If we neglect the friction  $F_m = F_L = 0$ , the eqn. (5) becomes:

$$\frac{\theta_m(s)}{T_e(s)} = \frac{1}{(J_m + J_L) s^2} \frac{1 + \frac{J_L}{K_o} s^2}{1 + \frac{J_m J_L}{K_o (J_m + J_L)} s^2}. \quad (6)$$

The transfer function (6) has a pair of non-damped conjugate complex poles:

$$p_{1,2} = \pm j \sqrt{(J_m + J_L) K_o / J_m J_L}, \quad (7a)$$

and a pair of non-damped conjugate complex zeros:

$$z_{1,2} = \pm j \sqrt{K_o / J_L}. \quad (7b)$$

This points to the possibility of occurrence of weakly damped oscillations in the moments of assigning of new values of reference moments. This phenomenon is particularly apparent in speed-controlled servomechanisms which use relatively long shafts for coupling with load, and has particularly negative effect to the performance of servo drives.

In cases when the shaft is short, the transfer function (6) can be additionally simplified. Putting  $K_o \rightarrow \infty$  in (6), one can obtain:

$$\frac{\mathcal{G}_m(s)}{T_e(s)} = \frac{1}{Js^2}, \quad (8)$$

where  $J = J_m + J_L$  is the total inertia of electrical drive and load. In the general case,  $J$  includes inertias of all rotational parts of the mechanical subsystem.

The structure shown in Fig 4 corresponds to the eqn. (8).

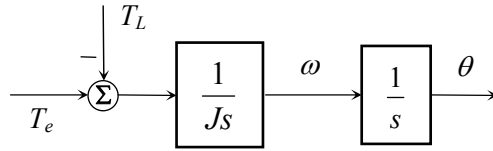


Fig. 4

The structure shown in Fig. 4 corresponds to the SIMULINK model shown in Fig. 4a.

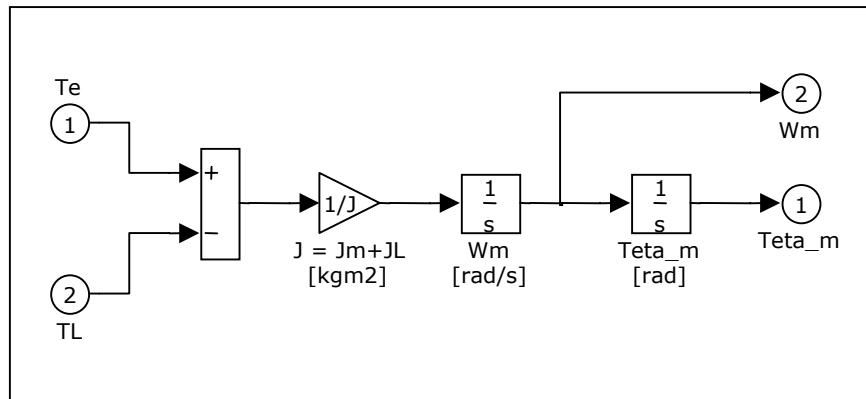


Fig. 4a

### 3.3 Electrical subsystem

The electrical subsystem of the speed-controlled servomechanism consists of:

- Drive converter (P),
- Electrical drive (M) as the actuator of electromagnetic moment.

Drive converter (P) generates a voltage at the connection ends of electrical drive (M) so that output moment  $T_e$  tracks reference input  $T_e^*$ . From the aspect of speed-controlled loop, it is desirable that the response of output moment  $T_e$  to step input has rising edge as fast as possible and lowest transport delay. In this manner, the negative effects of finite response rate of electrical subsystem to the dynamics of speed-controlled loop are minimized.

#### 3.3.1 Modeling of electrical subsystem in SIMULINK

The main characteristics of electrical subsystem having a pair of dominant complex conjugate poles, with small damping factor  $\xi$  and large pole frequency  $\omega_n$ , are fast rising edge and small transport delay. In this case, the transfer function of electrical subsystem is given by:

$$\frac{T_e(s)}{T_e^*(s)} = K_m \frac{\omega_n^2}{s^2 + 2\xi\omega_n s + \omega_n^2}, \quad (9)$$

where  $K_m$  is moment constant.

In nonlinear working regime of speed-controlled loop, which arises when drive converter (P) enters into saturation because of current limiting, the value of output moment  $T_e$  is limited to  $\pm T_{\max}$ .

The structure shown in Fig 5 corresponds to the eqn. (9).

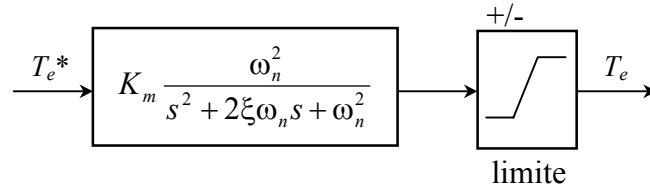


Fig. 5

The structure shown in Fig. 5 corresponds to the SIMULINK model shown in Fig. 5a.

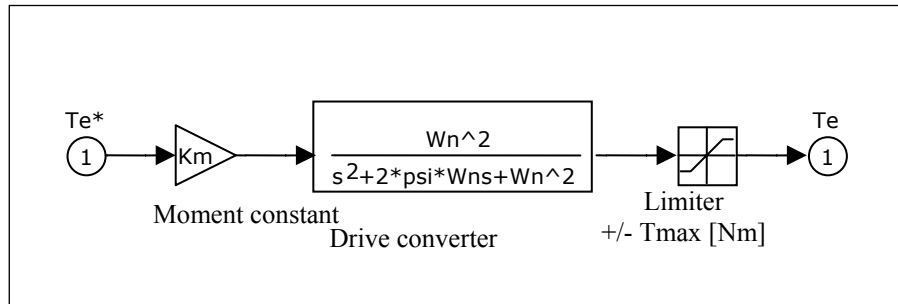


Fig. 5a

### 3.3.2 Delay of electrical subsystem

The transfer function introduces a delay which should be taken into account during structural synthesis of speed-controlled loop and when choosing the parameters of speed regulator. In contrary, in the response of regulated speed undesired overshoots will be noticed, and the system will be sensitive to the disturbances of moment load because of lower stability margin.

As the first approximation, the transfer function of electrical subsystem can be modeled by first order time delay

$$\frac{T_e(s)}{T_e^*(s)} \cong \frac{K_m}{1 + s\tau_e}, \quad (10a)$$

where  $\tau_e$  is the dominant time constant of electrical subsystem, given by:

$$\tau_e \leq \frac{1}{\xi\omega_n}. \quad (10b)$$



It remains to choose dominant time constant  $\tau_e$ .

*The dominant time constant  $\tau_e$  is chosen so that the delay of step response of electrical subsystem and the delay of step response of the first order model are equal.*

Remember that time delay is the time for which step response of the observed system reaches 50% of its nominal value.

The following computer simulation illustrates the effects of modeling the dynamics of electrical subsystem. In Fig. 6, it is shown:

- Step response of electrical subsystem (9) with parameters  $K_m = 1$ ;  $\xi = 0.3$ ;  $\omega_n = 1 \text{ rad/s}$ .
- Step response of first order model (10) with parameters  $K_m = 1$ ;  $\tau_e = 1/(2\xi\omega_n) = 1.7 \text{ s}$ .

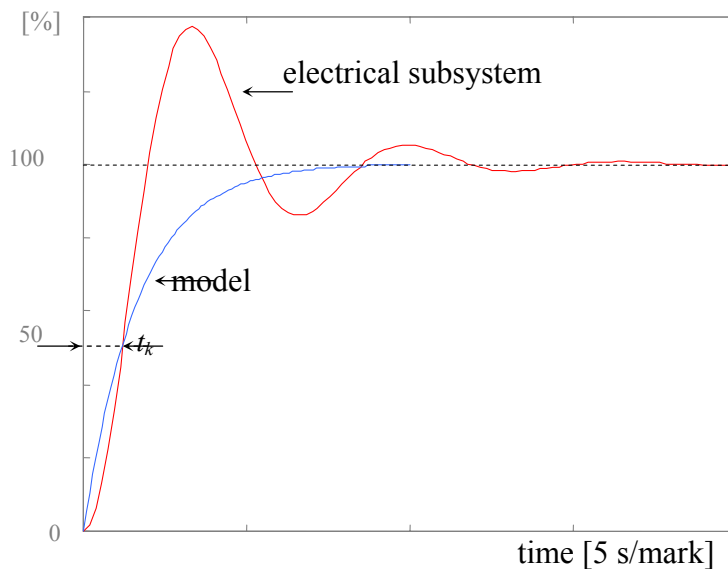


Fig. 6.

It should be noted that the time delay  $t_k$  of step response of electrical subsystem and time delay of step response of model are equal. In the procedure for optimal tuning of the parameters of speed regulator, the adopted model provides strict aperiodicity of regulated speed. Lower values of dominant time constant  $\tau_e$  have as the consequence the bandwidth of speed-controlled loop which “sees” overshoots of electrical subsystem and speed-controlled response, which is not strictly aperiodical. Higher values have as the consequence speed-controlled response, which is unnecessarily slow.

### 3.4 Sensor

Speed controlled servomechanisms having high quality dynamic behavior require high accuracy sensors for measuring position. In practice, two types of sensors are used:

- Optical encoders (absolute or incremental)
- Electromagnetic resolver with synchroconverter

### 3.4.1 Optical encoder

In absolute optical encoders, the position of motor's shaft is obtained by direct reading of coded position from disk. For coding, Gray or binary cyclic code is most often used, where coded values of two subsequent numbers differ in one bit only. In this way the error in angle detection is reduced, and it can be at most one increment of the detected quantity. The detected value must be converted from cyclic into natural binary code before entering into processor.

Incremental optical encoder is equipped with transparent disk onto which are deposited nontransparent dense equidistant markers. The light detector is used for reading of markers. During rotation of disk, the light detector generates the impulse train, which serves as the clock for a bi-directional counter. Each impulse of incremental encoder corresponds to an angle increment of one quant. In this way, the state of counter represents digital equivalent of position increment. By adding successive values of states of counter, one obtains the digital equivalent of the measured position.

The advantages of incremental encoders over the direct optical encoders are numerous, and as a rule they are used as sensors in servomechanisms with high quality dynamic behavior. First of all, the resolution of position measurement is significantly higher and it is limited by the spacing of transparent stripes on the disk. At present technology level, the resolution of position measurement in most incremental optical encoders is 10 or 12 bits. Also, the pulses coming from encoder can be used in capture-compare counter systems in digital controller for realization of advanced methods of speed measurements.

### 3.4.2 Modeling of optical encoder in SIMULINK

The process of converting of continuous position into its digital equivalent in encoder can be considered instantaneous because of high speed of electronic circuits. Because of this, for the model of optical encoder it is justified to use the transfer function

$$\frac{\theta_{out}}{\theta_{in}}(s) = K_n = \frac{2^N}{2\pi}, \quad (11)$$

where  $N$  is the number of bits in counter.

The structure shown in Fig 7 corresponds to the eqn. (11).

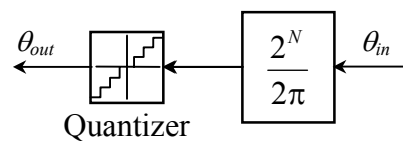


Fig. 7

The structure shown in Fig. 7 corresponds to the SIMULINK model shown in Fig. 7a.

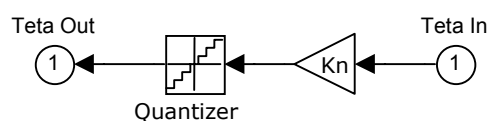


Fig. 7a.

Note: In the case of optical encoder (Fig. 7a), the block Quantizer takes the value 1.

### 3.4.3 Electromagnetic resolver with synchroconverter

In industrial environment, the sensor is exposed to oil vapors, dust, mechanical vibrations and high temperature, what makes impossible the use of optical encoders. In this environment, the robust electromagnetic resolver with synchroconverter is always used as sensor.

Electromagnetic resolver has the form of an electrical machine, which consists of rotational transformer, and detection set composed of *Sine* and *Cosine* detection windings. During rotation of motor shaft, because of high frequency excitation at the rotor (EXC), the analog voltages *sine* and *cosine* are induced in detection windings. Amplitudes and phases of these voltages contain information about the position of motor shaft. By using the radiometric method, on the basis of *sine* and *cosine* voltages the estimated position in digital form is obtained in the synchroconverter. The estimated position is located in bi-directional counter (Fig. 8) in the form of 10, 12, 14 or 16-bit digital word.

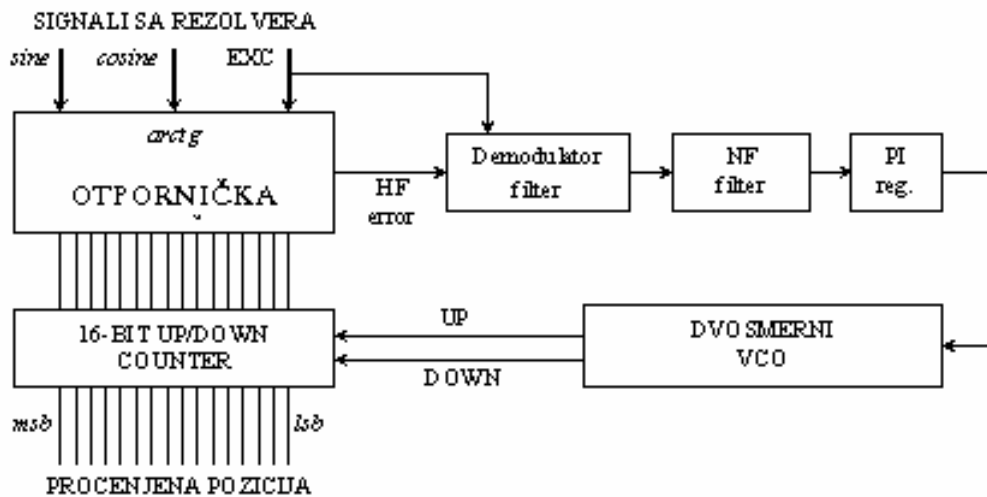


Fig. 8

The resistor network *arctg* at the input is organized so that a high frequency error signal appears at its output (HF error). This error is proportional to the difference between actual and estimated position, which is located in counter in digital form. High frequency error signal is first demodulated and then passed through a lowpass filter in order to be cleaned from high frequencies. The obtained analog signal is proportional to the difference between actual and estimated position, and it is brought into the regulator. The signal obtained at the output of the regulator is brought to the input of bi-directional voltage controlled oscillator (BVCO). The pulses generated at the output of BVCO converter (UP/DOWN) serve as the clock for a 16-bit counter, what provides that the estimated position tracks actual position of motor shaft.

### 3.4.4 Modeling of synchroconverter in SIMULINK

The transfer function of synchroconverter from the continuous input  $\theta_{in}$  to the digital output  $\theta_{out}$  is (Analog Devices, 2S82 R/D converter):

$$\frac{\theta_{out}}{\theta_{in}}(s_n) = K_n \frac{14(1+s_n)}{(s_n+2.4)(s_n^2+3.4s_n+5.8)}, \quad (12a)$$

where  $K_n$  is the transfer ratio of the synchroconverter:

$$K_n = p \frac{2^{16}}{2\pi}, \quad (p - \text{the number of pairs of resolver poles}) \quad (12b)$$

and where  $s_n$ , is the  $s$ -domain operator normalized by the passband edge frequency of synchroconverter  $f_{bw}$  [Hz].

$$s_n = \frac{2}{\pi \cdot f_{bw}} s = A_n s. \quad (12c)$$

The structure shown in Fig. 9 corresponds to the eqn. (12).

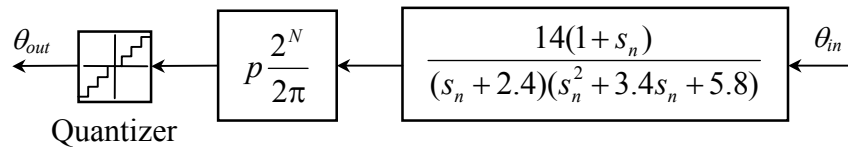


Fig. 9.

The structure shown in Fig. 9 corresponds to the SIMULINK model shown in Fig. 9a.

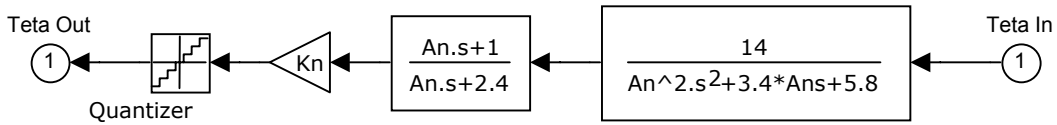


Fig. 9a.

**Note:** In the case of synchroconverter (Fig. 9a), the block Quantizer takes the value  $2^{16-N}$  where  $N$  is the resolution of the position measurement of the synchroconverter.

### 3.4.5 Delay of the synchroconverter

A delay should be added to the transfer function (12), which is needed in the structural synthesis of speed-controlled loop and during the choice of the parameters of the speed regulator. In contrary, in the response of the regulated speed some undesired overshoots will appear, and because of smaller stability margin the system will become sensitive to the influence of disturbances of load moment.

In the first approximation, the delay of synchroconverter can be modeled by first order time delay function:

$$\frac{\theta_{out}}{\theta_{in}}(s_n) \cong \frac{K_n}{1 + \tau_{rd}s}, \quad (13a)$$

where  $\tau_{rd}$  is the dominant time constant of the synchroconverter, given by:

$$\tau_{rd}[\text{s}] \cong \frac{1}{3f_{bw}[\text{Hz}]} \quad (13b)$$

The following computer simulation illustrates the effects of modeling of the dynamics of the synchroconverter. In Fig. 10 it is shown:

- step response of the synchroconverter (12) having parameters  $K_n = 1$ ,  $f_{bw} = 1$  kHz
- step response of the first order model (13) having parameters  $K_n = 1$ ,  $\tau_{rd} = 1/3$  ms.

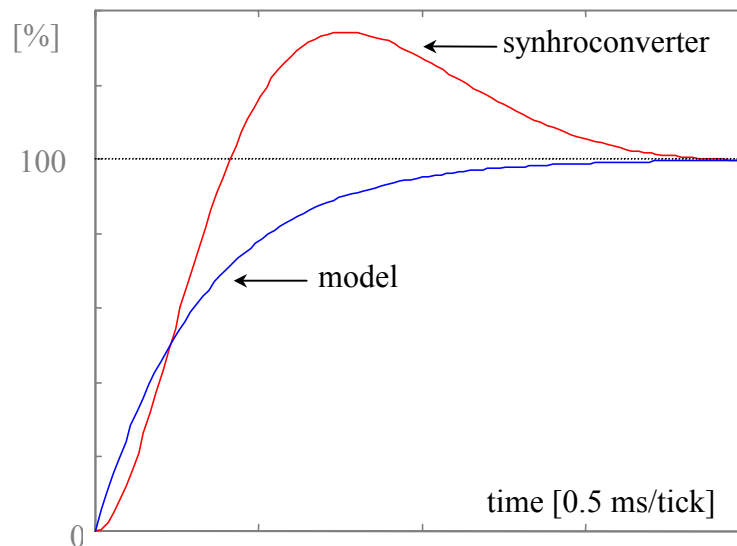


Fig. 10.

It should be noted that the settling times of step response of the synchroconverter and step response of the first order model are equal. In the procedure of optimal tuning of parameters of speed regulator (Section 3.7), the adopted model provides strict aperiodicity of the regulated speed. Smaller values of dominant time constant  $\tau_{rd}$  have as a consequence the bandwidth of the speed-controlled loop, which “sees” the overshoot of the synchroconverter, and the speed response which is not strictly aperiodical. Higher values of dominant time constant have as a consequence the speed response which is unnecessary slow.

### 3.5 Speed measurement block

In digitally controlled speed servomechanisms, the information about shaft speed is obtained in an indirect way. First, and most used method for speed measurement is the position difference method. By the use of sensor (D) the shaft position of electrical drive (EM) is measured, and by making difference of positions in discrete time instants with period  $T$ , the speed is determined as:

$$\omega(k) = \frac{\theta(k) - \theta(k-1)}{T}. \quad (14)$$

Applying the z-transform, the eqn. (14) becomes:

$$\omega(z) = \frac{1 - z^{-1}}{T} \theta(z). \quad (15)$$

The structure shown in Fig. 11 corresponds to the eqn. (15).

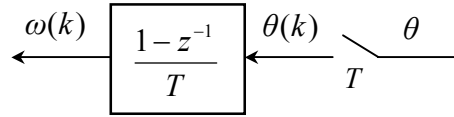


Fig 11.

Since first order derivative has high frequency character, the position difference is highly sensitive to the quantization of the position in sensor. As a result, the estimated speed at the output of the block for speed measurement can have only the values from the set:

$$\omega(k) = n \cdot \Delta\omega, \quad (n - \text{integer}) \quad (16a)$$

where  $\Delta\omega$  is one quant of speed given by:

$$\Delta\omega[\text{rad/s}] = \frac{\Delta\theta}{T} = \frac{2\pi}{2^N T}. \quad (16b)$$

As the consequence of (16), the ripple in **driving torque** appears, which has highly negative influence to performance of the servo drive. Peak-to-peak value of these oscillations, in the case of PI regulator from Fig. 14a, can be estimated from the expression:

$$\Delta m[\text{Nm}] \cong (K_p + K_i) K_n \Delta\omega \quad (17)$$

### 3.5.1 Modeling of speed measurement block in SIMULINK

The structure shown in Fig. 11 corresponds to the SIMULINK model shown in Fig. 11a.

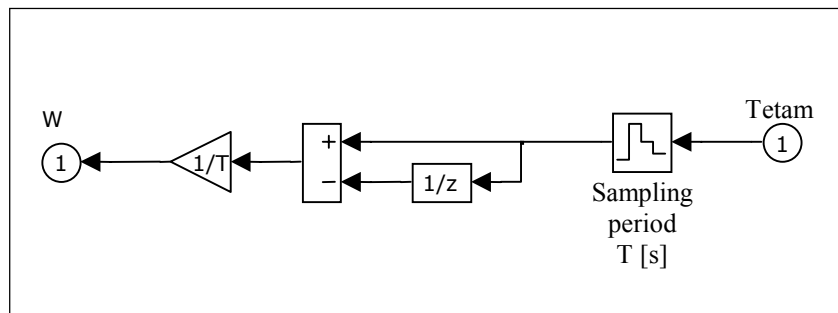


Fig. 11a.

### 3.6 Speed regulator

In many applications, it is required that under the constant reference input the static speed error should be zero, that the influence of constant drive moment to the accuracy of speed in steady

state conditions does not exist, and that response of speed to step response be strictly aperiodical having the settling time as small as possible.

First two requirements, which are related to the accuracy of regulated speed in steady state conditions, will be satisfied by the proper choice of the structure of speed regulator.

### 3.6.1 The choice of control structure of the speed regulator

A simplified model of speed-controlled loop, which can be used for the choice of control structure, is shown in Fig. 12. For the sake of simplicity, it is assumed that the coupling between electrical drive and load is **stiff**, and that there is no delay in the electrical subsystem. In the model shown in Fig. 12  $G(s)$  denotes the transfer function of the speed regulator which structure has to be determined.

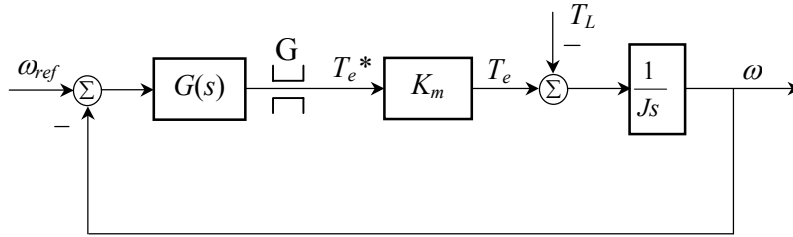


Fig. 12.

The regulation subsystem in Fig. 12 has only one **state** (because of mechanical inertia) so that the most simple proportional (P) speed regulator can be considered, which has the transfer function:

$$G(s) = K_p. \quad (18)$$

**The transfer function of the system in s-domain**, from the reference input  $\omega_{ref}$  and the disturbance  $T_L$  to the output  $\omega$  is

$$\omega(s) = \frac{CK_p}{s + CK_p} \omega_{ref}(s) - \frac{1}{J} \frac{1}{s + CK_p} T_L(s), \quad (19)$$

where  $C = K_m/J$  is the synthetic coefficient in which includes the parameters of the electrical and the mechanical subsystem. Since this is a first order system with time constant  $1/CK_p$ , each transitional effect, caused either by change of reference or by change of load, will be described by simple exponential law. However, this system does not have astaticism in relation to the disturbance, what points to the static error in the regulated speed when a constant **load torque affects the system**. In accordance to the limit theorem for the Laplace transform, the steady state value of the speed in the system with P regulator in Fig. 12, when the constant reference input  $\omega_{ref}(t) = \omega_{ref}h(t)$  and the constant load moment  $T_L = T_Lh(t)$  are in effect, is given by:

$$\omega(\infty) = \lim_{s \rightarrow 0} [s\omega(s)] = \omega_{ref} - \frac{T_L}{K_m K_p}, \quad (20)$$

and the error of speed by:

$$e(\infty) = \omega_{ref} - \omega(\infty) = \frac{T_L}{K_m K_p}. \quad (21)$$

In accordance with (21), the error of speed  $e(\infty)$  can be sufficiently reduced only if the gain  $K_p$  is made large. However, large value of the gain  $K_p$  corresponds to large values of the bandwidth of speed controlled loop ( $2\pi f_{bw} = CK_p$ ), so that it can happen that non-modeled dynamics leads out the system from the stable range. Besides that, it is not possible to realize large values of gain  $K_p$  without some problems in practice.

The static error of speed can be fully eliminated if the regulator with **proportional-integral** (PI) transfer function is used for the regulation of speed:

$$G(s) = K_p + \frac{K_i}{s}, \quad (22)$$

where  $K_p$  and  $K_i$  are the gains of proportional and integral actions, respectively.

With PI regulator, the transfer function from the reference input  $\omega_{ref}$  and the disturbance  $T_L$  to the output  $\omega$  is

$$\omega(s) = \frac{CK_p s + CK_i}{f_{PI}(s)} \omega_{ref}(s) - \frac{1}{J} \frac{s}{f_{PI}(s)} T_L(s), \quad (23a)$$

where  $f_{PI}(s)$  is the characteristic polynomial given by:

$$f_{PI}(s) = s^2 + CK_p s + CK_i. \quad (23b)$$

The system in Fig 12 with PI regulator has the needed degree of astatism related to the constant disturbance, so that in accordance to the limit theorem for the Laplace transform, the steady state value of the speed:

$$\omega(\infty) = \lim_{s \rightarrow 0} [s\omega(s)] = \omega_{ref}, \quad (24)$$

and the error of the speed,

$$e(\infty) = \omega_{ref} - \omega(\infty) = 0. \quad (25)$$

Therefore, the PI regulator makes possible the tracking of the constant reference input without static error when the system is excited by the constant or slow-variable load moment.

**Elimination of overshoot:** The existence of a finite zero in the transfer function (23a) points out that with the use of serial PI regulator it is not possible to achieve strictly aperiodical response, but the overshoot will be present in the speed response. The overshoot of speed can be avoided using a small modification of the PI regulator as shown in Fig. 13.

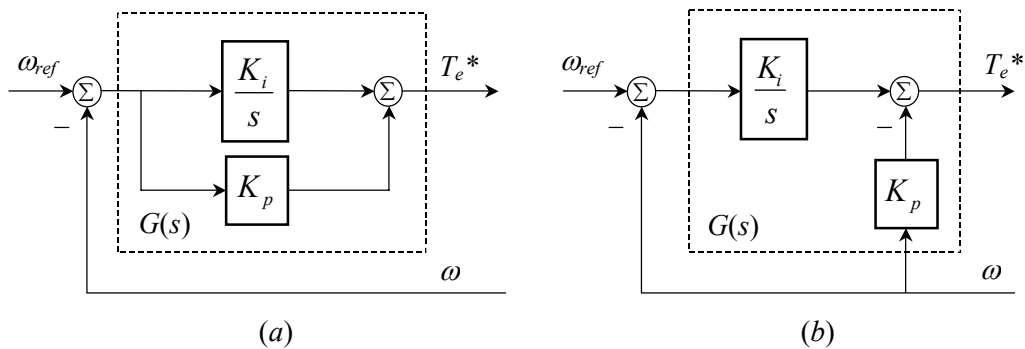


Fig. 13.



The modification consists of moving the P-action of speed regulation into the feedback path, what eliminates aforementioned finite zero. After this modification, the transfer function from the reference input  $\omega_{ref}$  and the disturbance  $T_L$  to the output  $\omega$  is

$$\omega(s) = \frac{CK_i}{f_{PI}(s)} \omega_{ref}(s) - \frac{1}{J} \frac{s}{f_{PI}(s)} T_L(s). \quad (26)$$

After moving the P-action, only the I-action is located in the path of error signal. In this way, the sudden jump of reference moment value  $T_e^*$  is avoided in the moments of assigning new values of reference inputs.

**Discretization:** The discrete version of transfer function  $G(s)$  is obtained by the discretization of the corresponding analog equivalent from Fig. 13. The modified PI regulator from Fig. 13b realizes the control law:

$$T_e^*(t) = K_i \int_0^t e(t) dt - K_p \omega(t), \quad (27)$$

where  $e(t) = \omega_{ref}(t) - \omega(t)$  is the error signal.

When the sampling period is small, the discrete equivalent of **control law** (27) can be obtained by an approximation of integral with a sum of rectangles of width  $T$  and height  $e(iT)$ , ( $i = 0, 1, 2, \dots$ ). So, it is obtained:

$$T_e^*(k) = K_i T \sum_{i=0}^k e(i) - K_p \omega(k). \quad (28)$$

The previous equation represents nonrecursive digital PI control law. From the aspect of program realization, it is more convenient to have recursive or incremental control law, which can be obtained first by changing  $k$  with  $k-1$  in (28)

$$T_e^*(k-1) = K_i T \sum_{i=0}^{k-1} e(i) - K_p \omega(k-1), \quad (29)$$

and later by subtracting (29) from (28). In this way, the digital incremental PI control law becomes:

$$\Delta T_e^*(k) = K_i T e(k) - K_p [\omega(k) - \omega(k-1)], \quad (30a)$$

where

$$\Delta T_e^*(k) = T_e^*(k) - T_e^*(k-1). \quad (30b)$$

By the application of the Z-transform, the equations (30) become

$$\Delta T_e^*(z) = K_i E(z) - K_p (1 - z^{-1}) \Omega(z) \quad (31a)$$

$$\Delta T_e^*(z) = (1 - z^{-1}) T_e^*(z), \quad (31b)$$

where  $K_p$  and  $K_i$  are the P-action and the I-action of the digital speed regulator, respectively.

The structure shown in Fig. 14 corresponds to the control law (31).

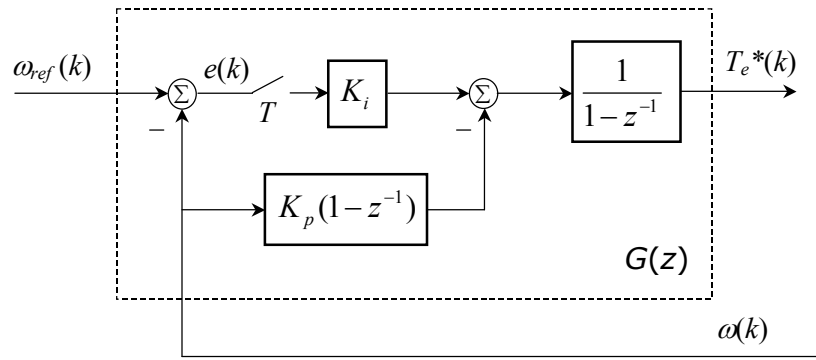


Fig. 14.

### 3.6.2 Modeling of speed regulator in SIMULINK

The structure shown in Fig. 14 corresponds to the SIMULINK model shown in Fig. 14a.

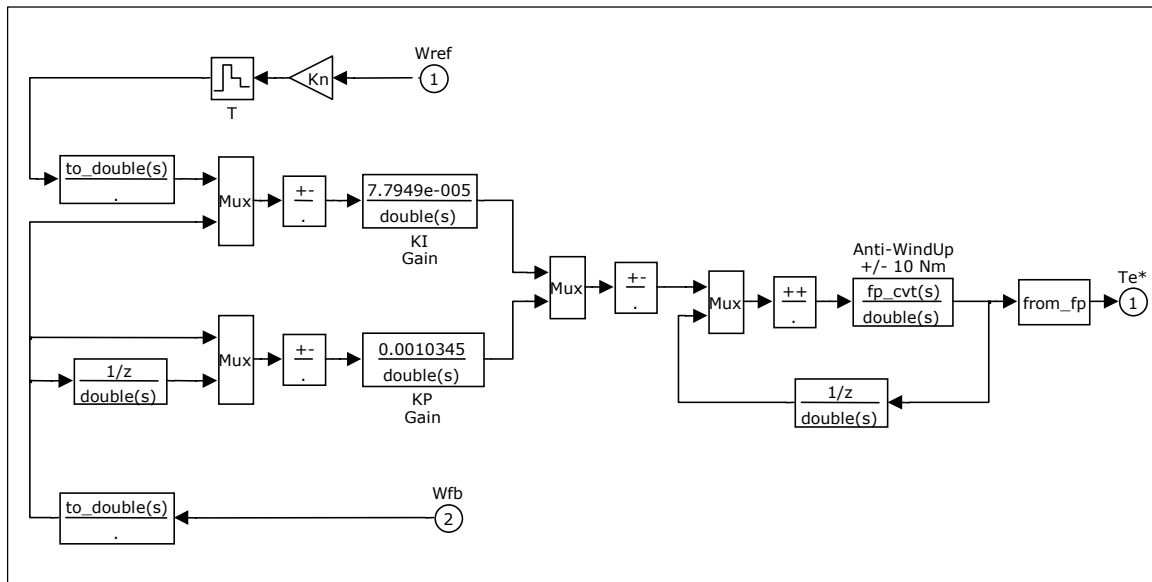


Fig. 14a.

It should be noted that the sensor ratio  $K_n$  is in the path of the reference input. This provides that the reference input has the same format as the processor's equivalent of speed, which comes from the block for speed measurement. The incremental form of the modified digital PI regulator is used for simple realization of the mechanism against filling up the integrator (anti-windup). The value in the integrator is limited so **that after the saturation takes place, further** increase of integral action is stopped. In this way undesired overshoots of drive moment and speed in nonlinear regime of speed loop are avoided.

For the realization of the model in Fig. 14a, the Fixed-Point Toolbox is used. This permits a detailed modeling of imperfections of digital processor, which realizes the function of speed regulator. For this purpose, the options *wsize*, *bp*, *rnd* and *check* are used. They define:

- *wsize* – the width of holding register (8, 16, or 32 bits)
- *bp* – the position of binary point related to the least significant bit
- *rnd* – the formation of the results (0 – truncation, 1 – rounding)
- *check* – working mode (0 – without overflow control, 1 – with overflow control)

These options do not have effect if the option *use floating-point* is used.

### 3.7 Optimal tuning of parameters of speed regulator

In Sections 3.3.2 and 3.4.5, it is shown that electrical subsystem and sensor (synchroconverter) have a **transport delay**. That's why it is necessary to take into account the delay which electrical subsystem and sensor introduce into speed controlling loop during the choice of parameters of the speed regulator. In contrary, some undesired overshoots will appear in the response of regulated speed, and the system will become to the influence of disturbances (of load moment) because of reduced stability margin.

The structure of a digitally regulated speed controlled servomechanism, which takes into account the delays of the electrical subsystem, and sensor is shown in Fig. 15.

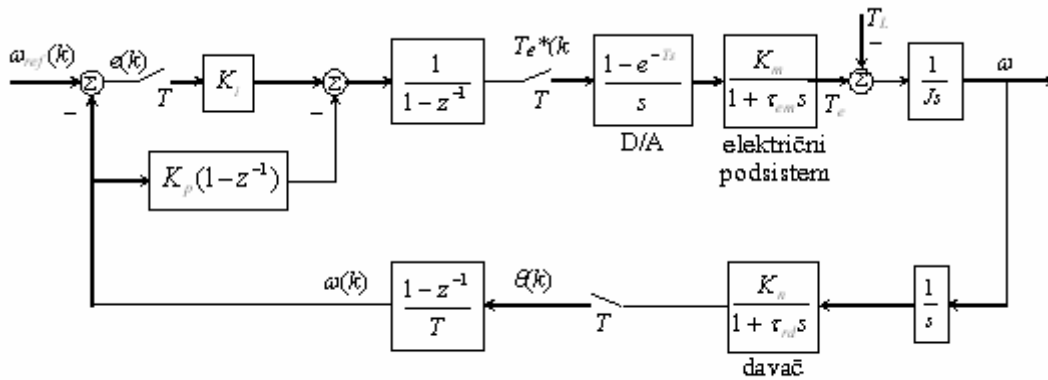


Fig. 15.

It is of some interest for further presentation to determine complex  $z$ -transform of error signal  $E(z)$  when system is excited by a step signal  $\Omega_{ref}(z) = \Omega_{ref} / (1 - z^{-1})$ . From structure block diagram in Fig. 15, for  $T_L = 0$ , it is obtained:

$$E(z) = \frac{z[z(z-1)(z-\beta) + K_p C(1-\beta)(z+1)]}{f(z)} \Omega_{ref}, \quad (33a)$$

where  $f(z)$  is the characteristic polynomial given by:

$$f(z) = z^3 + z^2[-2-\beta + (K_p C + K_i C)(1-\beta)] + z[1+2\beta + K_i C(1-\beta)] - K_p C(1-\beta) - \beta. \quad (33b)$$

and where  $C$  is the synthetic coefficient given by:

$$C = \frac{K_m K_n T}{2J}. \quad (33c)$$

In expression (33), the parameter  $\beta$  is given by:

$$\beta = \exp(-T/\tau), \quad (34)$$

where the time constant  $\tau$  is given by:

$$\tau = \sqrt{\tau_e^2 + \tau_{rd}^2}. \quad (35)$$

The desired character and dynamics of the speed-controlling loop in the linear regime is obtained by the proper adjustment of parameters of the speed regulator. Since adopted structure of speed regulator makes possible realization of strictly aperiodical response, without overshoots, the optimal values of parameters  $K_p$  and  $K_i$  can be determined by the minimization of the sum of error signal samples, that is by the optimization of system regarding the quality index of dynamic behavior.

$$J_e = \min \sum_{k=0}^{+\infty} e(kT). \quad (36)$$

Since the complex  $z$ -transform of error signal is by definition:

$$E(z) = \sum_{k=0}^{+\infty} e(kT)z^{-k}, \quad (37)$$

the quality index of dynamic behavior (36) can be computed as:

$$J_e = \min E(z) |_{z=1}. \quad (38)$$

By the use of (38) it is obtained:

$$J_e = \min \frac{2K_p C(1-\beta)}{f(1)} \Omega_{ref} = \min \frac{K_p}{K_i} \Omega_{ref}. \quad (39)$$

Therefore, the optimal tuning of control parameters  $K_p$  and  $K_i$  is reduced to the determination of the minimum of the ratio  $K_p/K_i$  under the condition that all zeros of the characteristic polynomial (33b) lay on the positive part of the real axis inside unit circle with center at the origin of the  $z$ -plane.

If  $\sigma_1$ ,  $\sigma_2$  and  $\sigma_3$  are zeros of the characteristic polynomial (33b), that is poles of the system with closed feedback loop, then the characteristic polynomial can be rewritten as:

$$f(z) = \prod_{i=1}^3 (z - \sigma_i) = z^3 - z^2(\sigma_1 + \sigma_2 + \sigma_3) + z(\sigma_1\sigma_2 + \sigma_1\sigma_3 + \sigma_2\sigma_3) - \sigma_1\sigma_2\sigma_3. \quad (40)$$

Equating the coefficients of the polynomials (33b) and (40), it is obtained:

$$\sigma_1 + \sigma_2 + \sigma_3 = 2 + \beta - (K_p C + K_i C)(1 - \beta) \quad (41a)$$

$$\sigma_1\sigma_2 + \sigma_1\sigma_3 + \sigma_2\sigma_3 = 1 + 2\beta + K_i C(1 - \beta) \quad (41b)$$

$$\sigma_1\sigma_2\sigma_3 = \beta + K_p C(1 - \beta) \quad (41c)$$

or, by adding equations (41),

$$\sigma_1\sigma_2\sigma_3 + \sigma_1\sigma_2 + \sigma_1\sigma_3 + \sigma_2\sigma_3 + \sigma_1 + \sigma_2 + \sigma_3 = 3 + 4\beta. \quad (42)$$

After the substitution of (33c) and (33b) in (39), the quality index of dynamic behavior can be expressed in dependence of poles of system with closed loop feedback as:

$$J_e = \frac{\sigma_1\sigma_2\sigma_3 - \beta}{\sigma_1\sigma_2 + \sigma_1\sigma_3 + \sigma_2\sigma_3 - 1 - 2\beta} \Omega_{ref}. \quad (43)$$

The necessary condition for the existence of the minimum of function (43) in the range  $0 < \sigma_i < 1$  is:

$$\frac{\partial J_e}{\partial \sigma_i} = 0, \quad (i = 1, 2, 3). \quad (44)$$

By finding these partial derivatives, a system of simultaneous equations is obtained, from which can be concluded that quality index of dynamic behavior  $J_e$  has the minimum value when poles of observed speed-controlled servomechanism are equal and lie inside unit circle in the  $z$ -plane. Putting  $\sigma_1 = \sigma_2 = \sigma_3 = \sigma_{opt}$  in (42), it is obtained:

$$\sigma_{opt} = \sqrt[3]{4 + 4\beta} - 1. \quad (45)$$

The optimal values of parameters  $K_p$  and  $K_i$  can be determined from the equations (41c) and (41b) respectively, if we make the change  $\sigma_1 = \sigma_2 = \sigma_3 = \sigma_{opt}$ . So, it is obtained:

$$K_p = \frac{\sigma_{opt}^3 - \beta}{(1 - \beta)C} \quad \text{and} \quad K_i = \frac{3\sigma_{opt}^2 - 1 - 2\beta}{(1 - \beta)C}. \quad (46)$$

The bandwidth of the speed-controlling loop, having the optimal values of the parameters of speed regulator, is given by the expression:

$$f_{bw}[\text{Hz}] = \frac{-\ln \sigma_{opt}}{2\pi T}. \quad (47)$$

In the case when  $\beta \rightarrow 0$  (for  $T/\tau \geq 6$ ), the expression (46) becomes:

$$K_p = \frac{0.2022}{C} \quad \text{and} \quad K_i = \frac{0.0337}{C}. \quad (48)$$

## 4. Preparation for experiment

For experiment, it is necessary to have a PC, MATLAB program (version 5.1 or higher), SIMULINK module Fixed-Point Toolbox, and set of files:

- SIMULINK model *A.mdl*
- MATLAB command files *startA.m* and *trace.m*.

*A.mdl* and *startA.m* are starting files, and during experiment the experimentator should make by himself the simulation models *B.mdl* and *C.mdl* and command files *startB.m* and *startC.m*.

In the following, the description of the SIMULINK model *A.mdl* and command files *startA.m* and *trace.m* is given, as well as the instructions for the creation of the SIMULINK models *B.mdl* and *C.mdl*, and command files *startB.m* and *startC.m*.

### 4.1 SIMULINK model *A.mdl*

This model consists of the following SIMULINK blocks:

- Mechanical subsystem **with stiff coupling** (Fig. 4a)
- Electrical subsystem (Fig. 5a)
- Sensor - encoder (Fig. 7a)

- Block for measurement of speed (Fig. 11a)
- Digital PI speed regulator (Fig. 14a)

It allows examination of dynamic performances of digitally controlled speed servomechanism by the computer simulations of:

- delay of electrical subsystem.

The simulation begin by running command file *startA.m* from the MATLAB command line:

```
startA <Enter>
```

The results of simulation, the waveforms of drive moment and speed, are simultaneously shown in MATLAB working environment by running command file *trace.m*:

```
trace <Enter>
```

**Note:** The SIMULINK model and command files must be in the MATLAB path.

## 4.2 SIMULINK model *B.mdl*

It should be created starting from model *A.mdl*. This model consists of the following SIMULINK blocks:

- Mechanical subsystem **with stiff coupling** (Fig. 4a)
- Electrical subsystem (Fig. 5a)
- Sensor - synchroconverter (Fig. 9a)
- Block for measurement of speed (Fig. 11a)
- Digital PI speed regulator (Fig. 14a)

It allows examination of dynamic performances of digitally controlled speed servomechanism by the computer simulations of:

- delay of electrical subsystem
- delay of sensor

The simulation begins by running command file *startB.m* from the MATLAB command line:

```
startB <Enter>
```

The command file *startB.m* is obtained when the block of instructions form command file *startA.m*:

```
%-----%
%Sensor - encoder
N = 12; % resolution [bits]
Kn = 2^N/(2*pi); % expression (11)
kvant = 1;
%-----%
%Dominant time constant
Tau = Te; % expression (35)
```

```
%-----%
```

is replaced by the following block of instructions:

```
%-----%
%Sensor - synchroconverter
N = 12; % resolution [bits]
Fbw = 1000; % bandwidth in [Hz]
kvant = 2^(16-N);
An = 2/(pi*Fbw); % expression (12c)
Kn = 2^16/(2*pi); % expression (12b)
Trd = 0.33/Fbw; % expression (13b)
%-----%
%Dominant time constant
Tau = sqrt(Te^2 + Trd^2); % expression (45)
%-----%
```

### 4.3 SIMULINK model *C.mdl*

It should be created starting from model *B.mdl*. This model consists of the following SIMULINK blocks:

- Mechanical subsystem **with elastic coupling** (Fig. 4a)
- Electrical subsystem (Fig. 5a)
- Sensor - synchroconverter (Fig. 9a)
- Block for measurement of speed (Fig. 11a)
- Digital PI speed regulator (Fig. 14a)

It allows examination of dynamic performances of digitally controlled speed servomechanism by the computer simulations of:

- delay of electrical subsystem
- delay of sensor
- elastic coupling

The simulation begins by running command file *startC.m* from the MATLAB command line:

```
startC <Enter>
```

The command file *startC.m* is obtained when the block of instructions from command file *startB.m*:

```
%-----%
%Parameters of mechanical subsystem with rigid coupling
Jm = 0.0008; % inertia of electrical drive in [kgm2]
JL = 0.0002; % inertia of load in [kgm2]
J = Jm + JL; % total inertia in [kgm2]
%-----%
```

is replaced by the following block of instructions:

```
%-----%  
%Parameters of mechanical subsystem with elastic coupling  
Jm = 0.0008;    % inertia of electrical drive in [kgm2]  
JL = 0.0002;    % inertia of load in [kgm2]  
J = Jm + JL;    % total inertia in [kgm2]  
Fm = 0.002;     % friction of electrical drive in [Nm/rad/s]  
FL = 0.002;     % friction of load in [Nm/rad/s]  
Ko = 350;       % rigidness of shaft in [Nm/rad]  
%-----%
```